Progress In Electromagnetics Research B, Vol. 44, 71–87, 2012

WIDEBAND DOUBLE-DIPOLE YAGI-UDA ANTENNA FED BY A MICROSTRIP-SLOT COPLANAR STRIPLINE TRANSITION

S. X. Ta[1], H. Choo[2], and I. Park[1, *]

[1]School of Electrical and Computer Engineering, Ajou University, Suwon, Korea

[2]School of Electronics and Electrical Engineering, Hongik University, Seoul, Korea

Abstract—This paper describes a wideband double-dipole Yagi-Uda antenna fed by a microstrip-slot coplanar stripline transition. The conventional dipole driver of a Yagi-Uda antenna is replaced by two parallel dipoles with different lengths to achieve multi-resonances, and a small, tapered ground plane is used to allow flexibility in the placement of a pair of reflectors for effective reflection of back-radiated electromagnetic waves. The measured bandwidth of the antenna was 3.48–8.16 GHz for a -10 dB reflection coefficient, with a flat gain of 7.4 ± 0.4 dBi. A two-element array of these antennas was also constructed, with a center-to-center spacing of 36 mm ($0.72\lambda_o$ at 6 GHz) and a common reflector between the elements. The two-element array had a measured bandwidth of 3.56–792 GHz, a gain of 8.40–10.43 dBi, a cross-polarization level of < -15 dB, and a mutual coupling of < -16 dB within the impedance-matching bandwidth.

1. INTRODUCTION

Quasi-Yagi antennas are widely utilized in many applications at microwave and millimeter-wave frequencies since it was first introduced in 1998 with remarkable features that included broad bandwidth, high efficiency, high gain, low profile, uniplanar structure, ease of fabrication, and low cost [1]. Quasi-Yagi antennas are fed by many different feeding structures, such as microstrip-lines (MS) [2–6], coplanar waveguides (CPW) [7], slotlines [8], MS-to-coplanar stripline (CPS) transitions [1, 9, 10], and CPW-to-CPS transformers [11, 12]. All

Received 6 August 2012, Accepted 11 September 2012, Scheduled 17 September 2012

* Corresponding author: Ikmo Park (ipark@ajou.ac.kr).

of the above antennas utilize a printed regular dipole as a driver, and have limited bandwidths that may be insufficient for multiple applications. To achieve multiband or wideband characteristics, the regular dipole driver of a Quasi-Yagi antenna can be modified into a variety of shapes, such as double dipoles [13–15], multi-branch dipoles [16, 17], bowtie dipoles [18, 19], or double-rhombus dipoles [20]. However, most of these antennas employ a large ground plane as a reflector, which cannot be well optimized for a radiation pattern like a conventional Yagi-Uda antenna. Recently, CPS-fed planar Yagi-Uda antennas [21, 22] have been introduced in the absence of a large ground plane, but these antennas are not suitable for array applications because of their feed structure.

This paper introduces a double-dipole Yagi-Uda antenna and a two-element array of these antennas, both exhibiting wide bandwidth and flat gain. The antenna is fed by a microstrip-slot coplanar stripline transition that utilizes a microstrip radial stub and a slot radial stub each with the same 90° angle, but with different radii [23] for wideband impedance matching. The ground plane is tapered to allow flexibility in the placement of a pair of reflectors, so that the controllability of the radiation pattern can be improved.

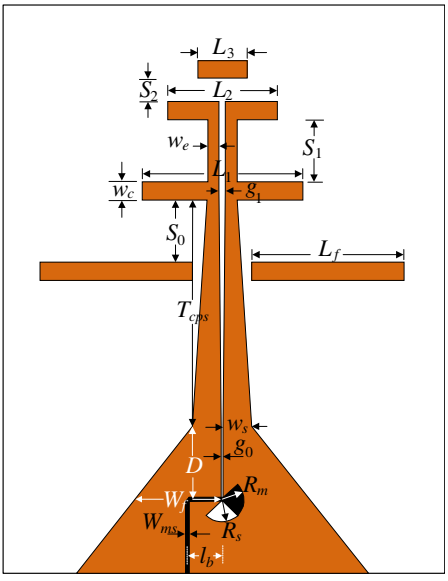

Figure 1. Geometry of the single antenna structure.

2. SINGLE ANTENNA

Figure 1 shows the geometry of the wideband double-dipole Yagi-Uda antenna structure, which was designed on a 60×80 mm RT/Duroid 6010 substrate with a dielectric constant $\varepsilon_r = 10.2$ and a thickness $t = 0.635$ mm. The antenna is comprised of a microstrip-coplanar stripline transition feed, a pair of reflectors, two parallel printed dipoles, and a parasitic strip as a director. A microstrip-slot coplanar stripline transformer is utilized as the transition feed. The microstrip-line was designed on the back side of the substrate with a characteristic impedance of $50\,\Omega$, and the slotline was designed on the front side of the substrate with a characteristic impedance of approximately $70\,\Omega$. A microstrip radial stub and a slot radial stub, both at 90°, but with different radii, are inserted into the transition for impedance matching between the microstrip-line and the slotline. The ground plane is gradually tapered to form the slotline-to-coplanar stripline transformer. At roughly the midpoint between the transition feed and the first parallel dipole, a pair of parasitic strips is arranged on both sides of the coplanar stripline for effective reflection of back-radiated electromagnetic waves. The antenna allows flexibility in the placement of the reflectors, owing to the absence a large ground plane, and thus the controllability of the radiation pattern is greatly improved. Two parallel dipoles with different lengths are utilized as the primary radiation elements to achieve multi-resonances, and are connected to the transition feed by a coplanar stripline. Since the input impedance of the parallel dipoles is higher than the characteristic impedance of the coplanar stripline at the transition ($\sim 70\,\Omega$), a section of coplanar stripline between the transition feed and the parallel dipoles is tapered to improve the impedance-matching conditions.

An Ansoft high-frequency structure simulator (HFSS) was used to investigate the characteristics of the proposed antenna. Optimized antenna design parameters were chosen for an objective of wide bandwidth and small gain variation, as follows: $W_{ms} = 0.56$ mm, $l_b = 5$ mm, $W_f = 11.5$ mm, $R_s = 2.8$ mm, $R_m = 3.0$ mm, $D = 10$ mm, $g_0 = 0.2$ mm, $g_1 = 0.8$ mm, $w_s = 4.0$ mm, $w_e = 1.6$ mm, $T_{cps} = 32$ mm, $L_f = 21$ mm, $L_1 = 22$ mm, $L_2 = 15$ mm, $L_3 = 8$ mm, $S_0 = 12.6$ mm, $S_1 = 9.6$ mm, $S_2 = 2.5$ mm, and $w_c = 2.4$ mm. From the simulations, it was found that the lengths of the parallel dipoles and the director (L_1, L_2, and L_3) primarily determine the resonant frequencies of the antenna. The impedance matching conditions were obtained by altering the parameters of the tapered coplanar stripline section, wide line width (w_s) with small gap (g_0) to narrow line width (w_e) with large gap (g_1), between the transition feed and the parallel dipoles. The

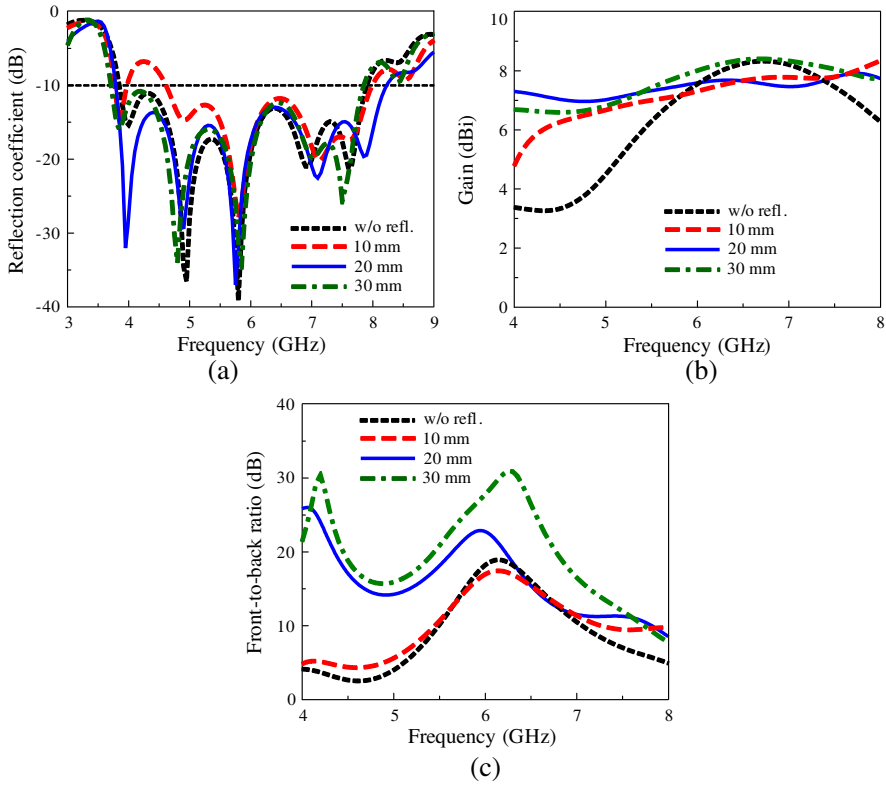

Figure 2. Simulated (a) reflection coefficient, (b) gain, and (c) front-to-back ratio as functions of frequency for various reflector lengths (L_f).

effect of these parameters on the variation of the radiation pattern was negligible. In the following paragraphs, the antenna design parameters that strongly affect the radiation characteristics are studied; each parameter is varied while keeping the other parameters fixed, as listed above.

Figure 2 shows the antenna characteristics as functions of the reflector length (L_f). As shown in Fig. 2(a), the resonant frequencies varied insignificantly both with and without reflectors in all cases. When L_f increased from 0 to 20 mm, the gain and front-to-back ratio improved significantly in the low-frequency region, but varied slightly in the high-frequency region [Figs. 2(b), 2(c)]. When $L_f \geq 20$ mm, the gain was relatively stable [Fig. 2(b)], whereas the front-to-back ratio increased at 4–8 GHz range [Fig. 2(c)]. The minimum gain variation was obtained with a reflector length of approximately 20 mm, as shown

in Fig. 2(b). These observations indicate that the reflector length primarily affects the radiation characteristics of the antenna, and the optimum result in terms of minimum gain variation was obtained when the reflector length was approximately equal to one-half the effective wavelength at the lowest resonant frequency ($\lambda_{eff} \sim 21$ mm).

The proposed antenna employs a pair of parasitic strips as the reflectors. Therefore, the radiation characteristics of the antenna can be easily controlled by arranging the reflecting elements with an insignificant change of the impedance matching bandwidth. This is shown in Fig. 3, which plots the simulated reflection coefficient, gain, and front-to-back ratio as functions of the frequency for various values of the space between the reflectors and the longer of the parallel dipoles (S_0). As S_0 was increased from 7.6 to 17.6 mm in 5-mm increments, the following antenna characteristics were observed; the

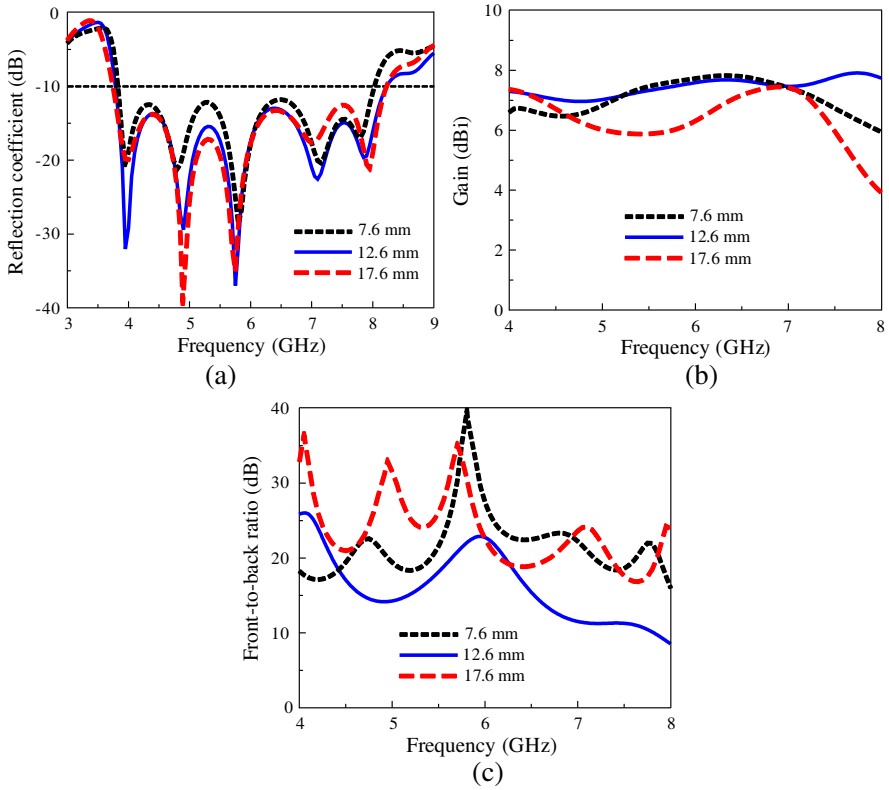

Figure 3. Simulated (a) reflection coefficient, (b) gain and (c) front-to-back ratio as functions of frequency for various values of the space between the reflectors and the longer of the parallel dipoles (S_0).

wide impedance matching bandwidth unaffected [Fig. 3(a)] while the 12.6 mm space offered the highest gain and minimum gain variation at 4–8 GHz [Fig. 3(b)], but exhibited the smallest front-to-back ratio in almost the 4–8 GHz range [Fig. 3(c)]. In the proposed antenna structure, the longer of the parallel dipoles (L_1) is not only a radiation element, but also acts as a reflector for the shorter of the parallel dipoles (L_2) in the high-frequency region. This is clearly shown in Fig. 4, which plots the simulated reflection coefficient, gain and front-to-back ratio as functions of frequency for various values of the space between the parallel dipoles (S_1). As S_1 was varied from 7.6 to 11.6 mm in 2-mm steps, the lower resonant frequencies decreased while the higher resonances hardly changed, as shown in Fig. 4(a). The gain improved slightly in the low-frequency region, but significantly decreased in the high-frequency region, as shown in Fig. 4(b). The front-to-back ratio

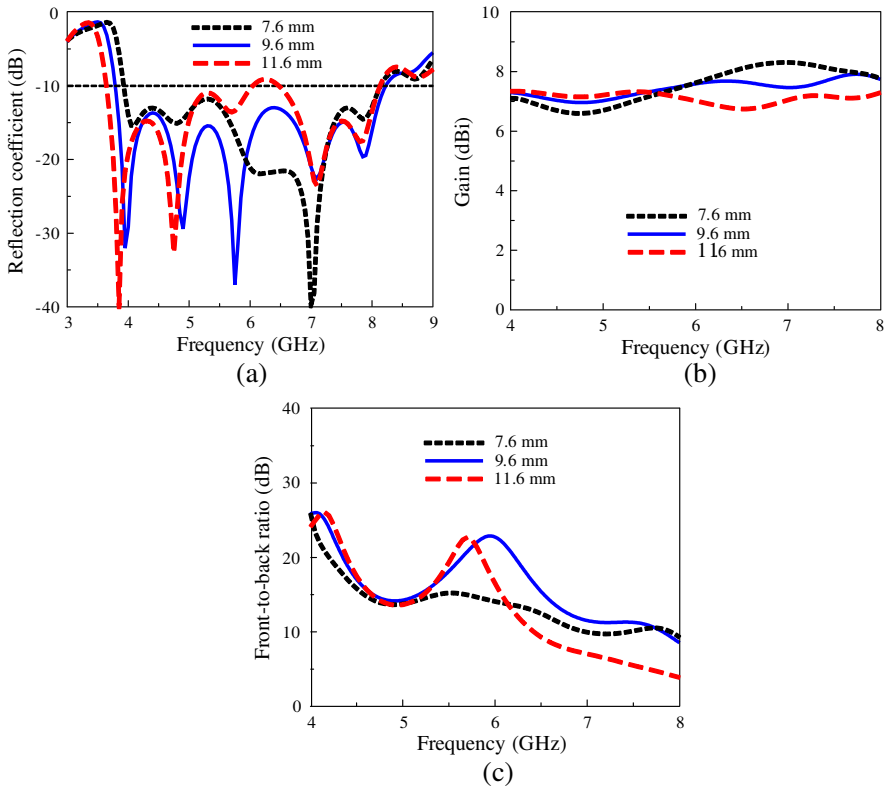

Figure 4. Simulated (a) reflection coefficient, (b) gain, and (c) front-to-back ratio as functions of frequency for various values of the space between the parallel dipoles (S_1).

varied considerably in the frequency region near 6 GHz, but hardly changed in the remaining regions, as shown in Fig. 4(c). These figures indicate that the radiation characteristics of the antenna can be optimized by adjusting the arrangement of the reflectors and the space between the parallel dipoles.

The antenna characteristics as functions of frequency for various values of the space between the shorter of the parallel dipoles and the director (S_2) are shown in Fig. 5. When this space was increased from 1.5 to 3.5 mm in 1-mm increments, the following antenna characteristics were observed; there were significant changes in both the reflection coefficient [Fig. 5(a)] and the gain [Fig. 5(b)] in the high-frequency region, but negligible changes in the low-frequency region, while the front-to-back ratio hardly affected at 4–8 GHz [Fig. 5(c)]. This indicates that the space between the shorter of the parallel dipoles

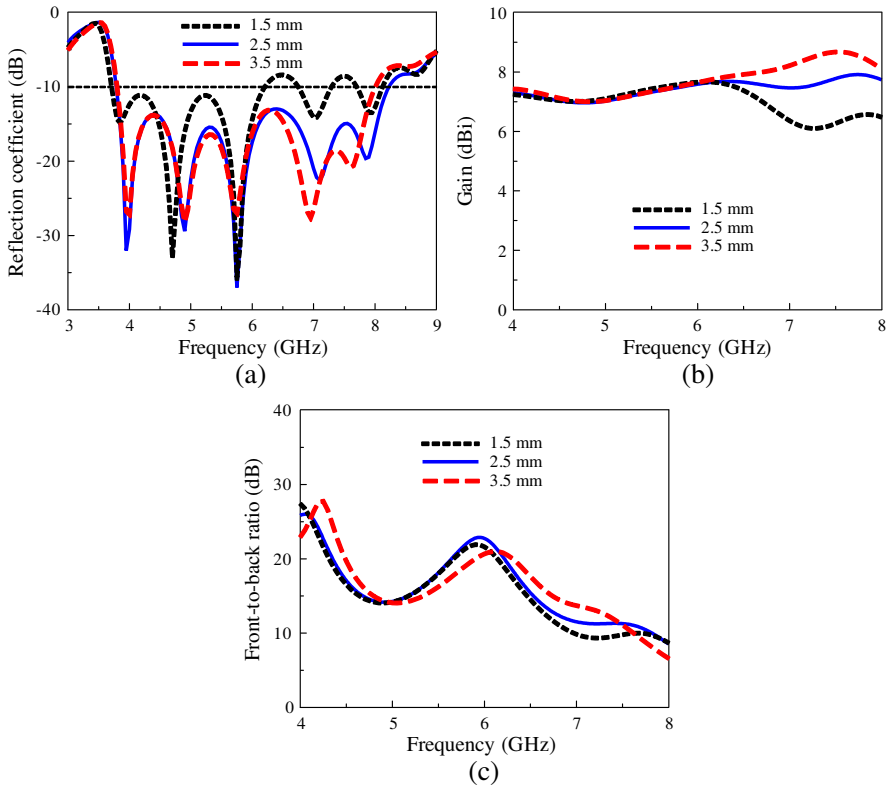

Figure 5. Simulated (a) reflection coefficient, (b) gain, and (c) front-to-back ratio as functions of frequency for various values of the space between the shorter of the parallel dipoles and the director (S_2).

and the director primarily affects the antenna characteristics in the high-frequency region.

The antenna was fabricated on both sides of an RT/Duroid 6010 substrate with a copper thickness of 20 μm, using a standard etching technology. A subminiature type-A (SMA) connector was used as the microstrip-to-coaxial line transition (not included in the HFSS simulations). An Agilent N5230A network analyzer and an Agilent 3.5-mm 85052B calibration kit were used for measuring the prototype [Fig. 6(a)]. Fig. 6(b) indicates good agreement between the simulated and measured reflection coefficients of the optimized antenna, with measured and simulated bandwidths of 3.48–8.16 GHz and 3.74–8.0 GHz, respectively, for the −10 dB reflection coefficient. The slight difference between the measured and simulated results could be attributed to a misalignment at the transition feed and the effect of the SMA connector.

The radiation patterns and the gain of the antenna were measured using an Agilent Vector Network Analyzer (E8362B). A standard horn antenna was utilized for transmitting and the proposed antenna for receiving. The distance between the transmitting and receiving antennas was 10 m. During the measurement process, the standard horn antenna was fixed and the Yagi-Uda antenna was rotated from −180° to 180°, with a scan angle of 1° and a speed of 3°/s. The measured 4, 6, and 8 GHz radiation patterns of the antenna were in close agreement with the HFSS simulation, as shown in Fig. 7, and exhibited a low cross-polarization level and symmetric profiles. At a frequency of 4 GHz, the measurements yielded half-power beamwidths

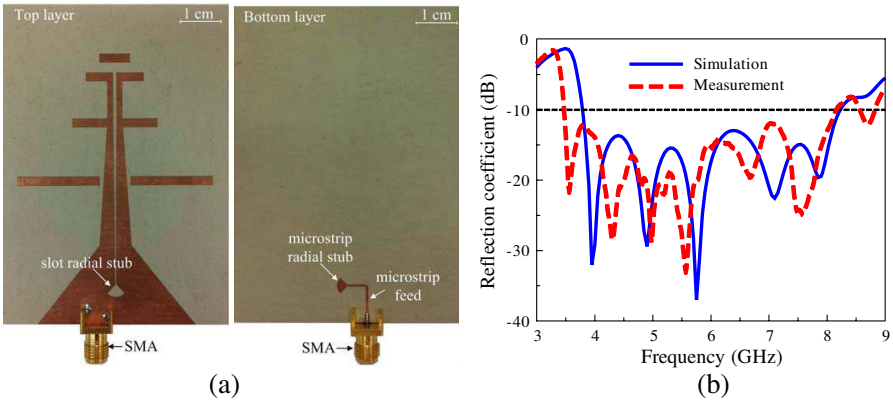

Figure 6. (a) Fabricated wideband double-dipole planar Yagi-Uda antenna, and (b) simulated and measured reflection coefficient.

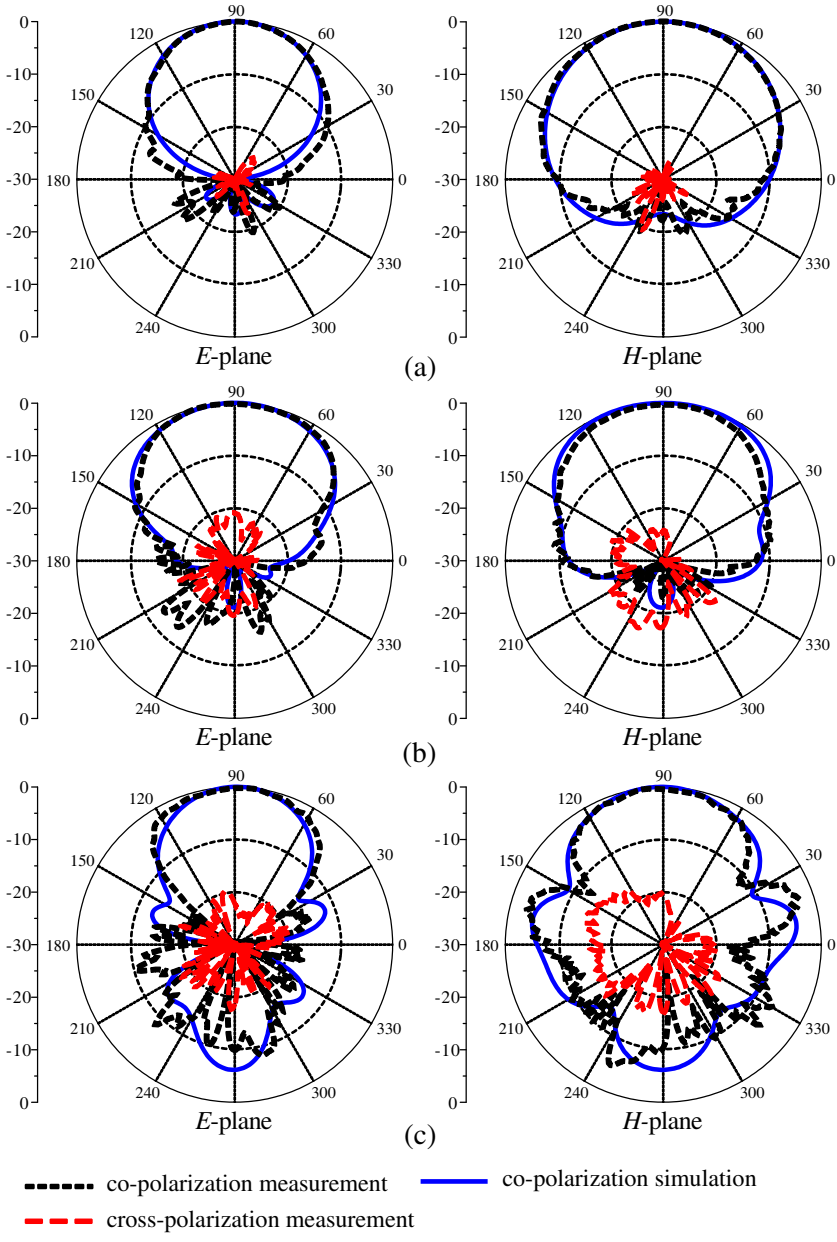

Figure 7. Radiation patterns of the antenna at (a) 4, (b) 6, and (c) 8 GHz. Simulated cross-polarization is excluded because the value is too small to show in the figure.

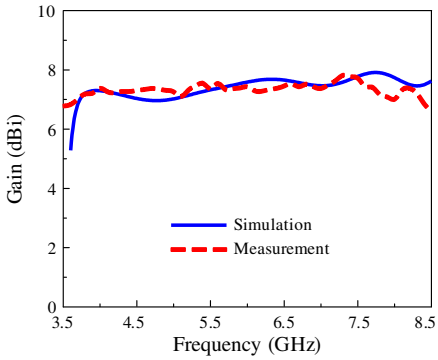

Figure 8. Measured and simulated gain of the antenna.

(HPBWs) of 72° and 117° in the E- and H-planes, respectively. At 6 GHz, the measurements yielded HPBWs of 90° and 95° in the E- and H-planes, respectively. At 8 GHz, the measurements yielded HPBWs of 73° and 80° in the E- and H-planes, respectively. As Fig. 8 shows, the measured gain of the antenna was 7.01–7.82 dBi throughout the impedance-matching bandwidth, and agreed well with the simulated gain of 7.0–7.9 dBi. Fig. 8 also indicates a small gain variation for the antenna across its bandwidth: the measured gain variation was ±0.4 dB and the simulated gain variation was ±0.45 dB. For a better understanding of the advantage of our antenna design, the performance comparisons between the proposed Yagi-Uda antenna and the previously reported wideband antennas are presented in Table 1. The proposed design exhibits a higher gain and a smaller gain variation as compared with the other antenna designs. The small gain variation ensures stable operation in wideband wireless communications.

3. TWO-ELEMENT ARRAY

It is well known that the mutual coupling is a common problem in the antenna arrays. It significantly affects the performance of almost all types of antenna array and is directly proportional to the spacing between the elements. In practice, many applications of planar antenna array require a mutual coupling ($|S_{21}|$) less than −15 dB in the entire operating bandwidth to avoid the undesired effects. Therefore, a two-element array of the proposed wideband double-dipole Yagi-Uda antennas was designed, based on a compromise between low mutual coupling and moderate spacing. The mutual coupling was first computed via HFSS simulation, with a center-to-center spacing

Table 1. Comparison between the proposed antenna and previously reported planar wideband antennas.

Single -element	Bandwidth (GHz)	Gain range (dBi)	Gain variation (dB)	Average gain (dBi)
Proposed	3.48–8.16 (80.4%)	7.01–7.82	0.81	7.4
Ref. [14]	5.5–14.2 (88%)	4.7–7.1	2.4	6
Ref. [18]	5.3–14.2 (91%)	—	—	6
Ref. [19]	1.32–3.39 (87.8%)	5.2–9.3	4.1	7.1
Ref. [20]	5.7–17.8 (103%)	4–9	5	6
Ref. [21]	3.9–5.9 (40.8%)	6.5–8.0	1.5	7.1

of 36 mm ($0.72\lambda_o$ at 6 GHz) in the presence of a common reflector (L_c) between the two antennas. As Fig. 9(a) shows, the mutual coupling at 4 GHz was greater than -15 dB for the original value of $L_c = 27.8$ mm, but could be improved by reducing the length of the common reflector. Unfortunately, the improvement in the mutual coupling was accompanied by a degradation of the gain of the two-element array, as shown in Fig. 9(b). Therefore, the final design of the array was given a center-to-center spacing of 36 mm with $L_c = 20$ mm for effective reflection of back-radiated electromagnetic waves, and to ensure that $|S_{21}| < -15$ dB within the impedance-matching bandwidth. The mutual coupling was determined by measuring the transmission coefficient ($|S_{21}|$) of the array with two ports of the Agilent N5230A network analyzer. The measurements agreed well with the HFSS simulation, and yielded a mutual coupling of < -16 dB at 3.5–4.5 GHz, and < -20 dB in the remaining regions of 3–9 GHz, as shown in Fig. 9(c).

A two-element array uses a T-junction power divider as the feeding network, which was also built on RT/Duroid 6010 substrate with a dielectric constant $\varepsilon_r = 10.2$ and a thickness $t = 0.635$ mm, shown in Fig. 10(a). The feeding network was designed to have an input impedance of 50 Ω, and was comprised of a 50–25 Ω wideband microstrip-line transformer. The transformer was tapered from narrow line width ($Z_o = 50\,\Omega$) to wide line width ($Z_o = 25\,\Omega$) before the

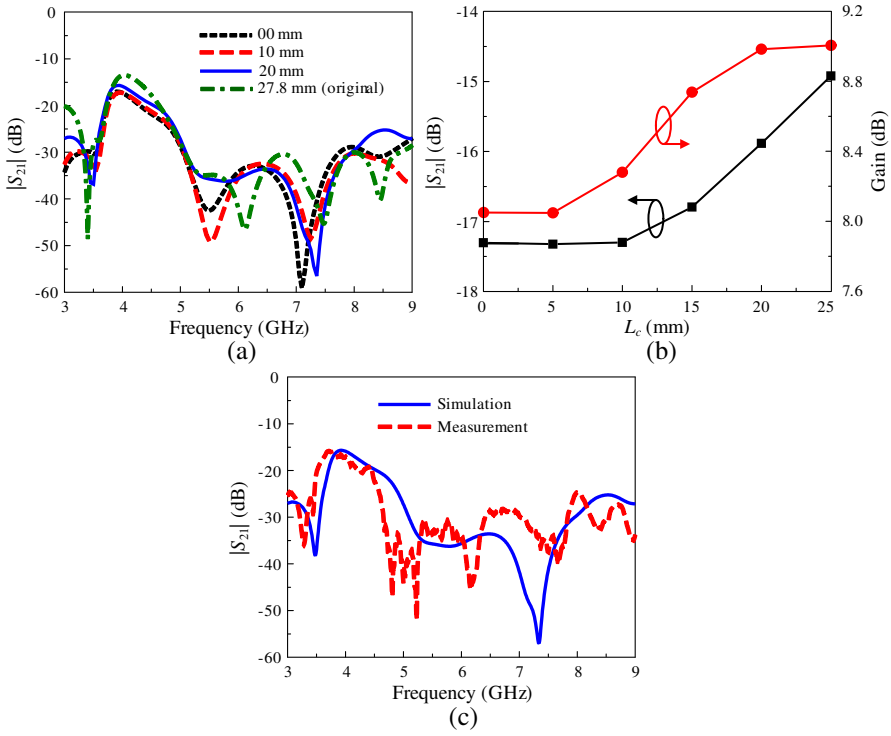

Figure 9. Two-element array with a center-to-center spacing of 36 mm ($0.72\lambda_o$ at 6 GHz): (a) simulated mutual coupling $|S_{21}|$ as a function of frequency for various common reflector lengths L_c, (b) simulated mutual coupling and gain at 4 GHz as a function of common reflector length L_c, (c) measured and simulated mutual coupling $|S_{21}|$ as a function of frequency.

microstrip-line was divided into two branches. Fig. 10(b) shows the simulated S-parameters of the T-junction power divider; the reflection coefficient ($|S_{11}|$) at Port 1 was better than -15 dB at 4–8 GHz. The transmission coefficient ($|S_{21}|$ or $|S_{31}|$) from Port 1 to Port 2 (or Port 3) was approximately 3.5 dB throughout 3–9 GHz. These results ensure that the loss at the feeding network of the array is insignificant. The two-element array of double-dipole Yagi-Uda antenna, as shown in Fig. 11(a), was fabricated and measured. The antenna had a common reflector length of $L_c = 20$ mm and a center-to-center spacing of 36 mm ($0.72\ \lambda_o$ at 6 GHz) between the elements. As Fig. 11(b) shows, the measured and simulated reflection coefficients of the two-element array agreed rather closely. The measured and simulated bandwidths for the

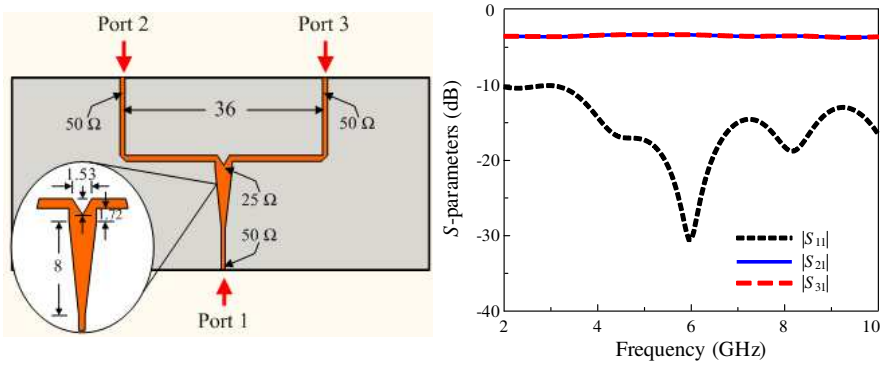

(a) (b)

Figure 10. (a) T-junction power divider geometry (units in mm) and (b) simulated S-parameters.

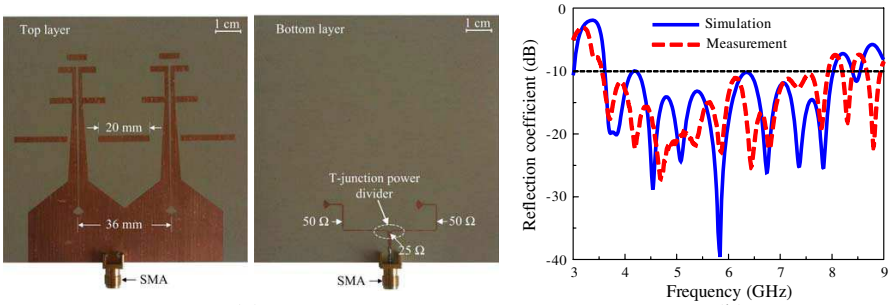

(a) (b)

Figure 11. (a) Fabricated two-element array with a center-to-center spacing of 36 mm ($0.72\lambda_o$ at 6 GHz), and (b) measured and simulated reflection coefficient as a function of frequency.

-10 dB reflection coefficient were 3.56–7.92 GHz and 3.69–8.23 GHz, respectively. The radiation patterns of two-element array at 4, 6, and 8 GHz are shown in Fig. 12. Again, the measured radiation patterns agreed well with the HFSS simulation. The measured and simulated HPBW ranged from 40–58° and 38–54°, respectively, in the E-plane, while the H-plane patterns of the array were almost the same as the H-plane patterns of the single antenna. In addition, the measurements yielded a stable radiation pattern with a low cross-polarization level (< -15 dB) and low side lobes (< -10 dB). Fig. 13 shows the measured gain of the two-element array, which ranged from 8.40–10.43 dBi, and agreed well with the simulated gain of 8.50–10.83 dBi throughout the impedance-matching bandwidth. A performance comparison between the two-element array of the proposed Yagi-Uda antenna and the two-element array in the previous reports is shown in Table 2.

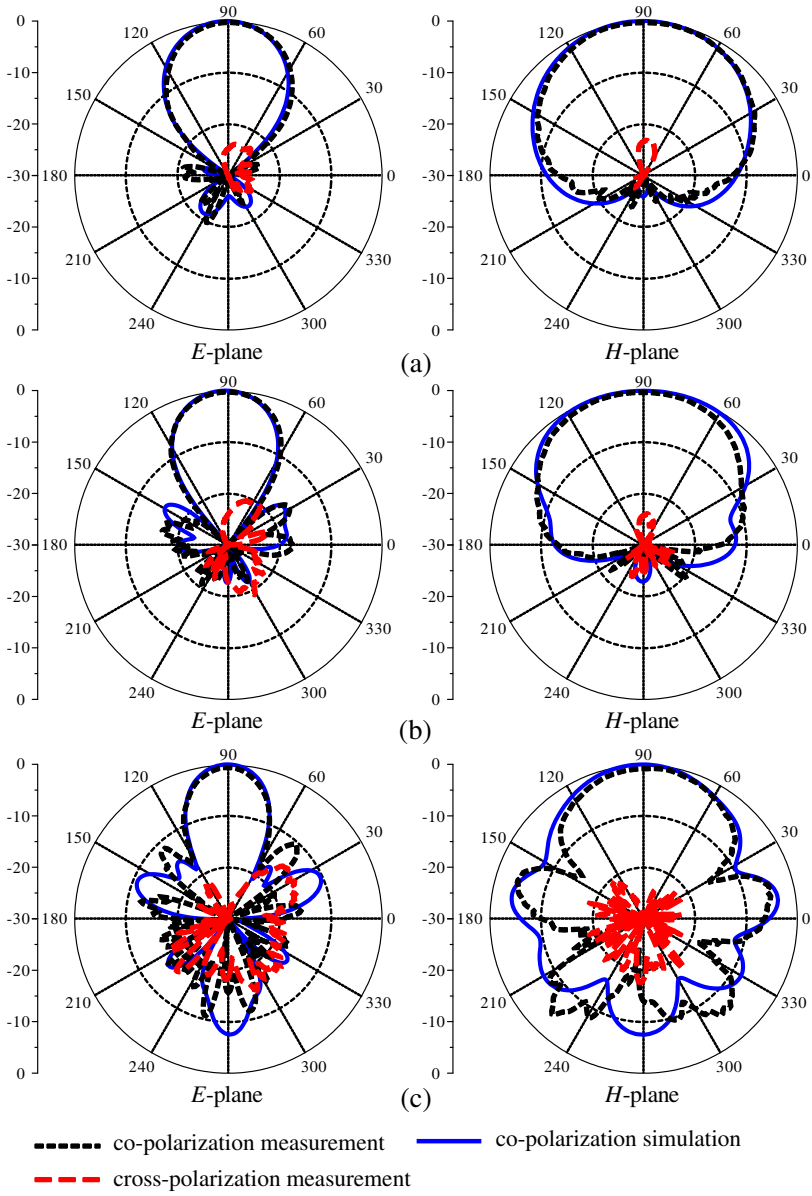

Figure 12. Radiation patterns of the two-element array at (a) 4, (b) 6, and (c) 8 GHz. Simulated cross-polarization is excluded because the value is too small to show in the figure.

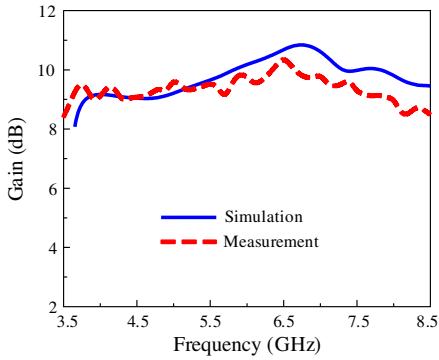

Figure 13. Measured and simulated gain of the two-element array.

Table 2. Comparison between the proposed two-element array and the previously reported two-element arrays.

Two-element array	Bandwidth (GHz)	Gain range (dBi)	Gain variation (dB)	Average gain (dBi)
Proposed array	3.56–7.92 (76%)	8.4–10.43	2.03	9.5
Ref. [14]	5.5–13.5 (84%)	5.5–9.4	3.9	8
Ref. [20]	5.7–16 (95%)	7–10.5	3.5	8.4

4. CONCLUSION

This paper introduced a wideband double-dipole Yagi-Uda antenna and a two-element array of these antennas, both exhibiting wide impedance-matching bandwidth and flat gain. The antenna allowed flexibility in the placement of reflectors, owing to the absence of a large ground plane, and thus the controllability of the radiation pattern was greatly improved. Two parallel dipoles with differing lengths were utilized as the primary radiation elements for the wideband characteristics. With its many advantages, this antenna could be widely applicable to wideband wireless communication systems.

REFERENCES

1. Qian, Y., W. R. Deal, N. Kaneda, and T. Itoh, "Microstrip-fed quasi-Yagi antenna with broadband characteristics," *Electronics Letters*, Vol. 34, No. 23, 2194–2196, Nov. 1998.

2. Zheng, G., A. A. Kishk, A. W. Glisson, and A. B. Yakovlev, "Simplified feed for modified printed Yagi antenna," *Electronics Letters*, Vol. 40, No. 8, 464–466, Apr. 2004.
3. Alhalabi, R. and G. Rebeiz, "High-gain Yagi-Uda antennas for millimeter-wave switch-beam systems," *IEEE Transactions on Antennas and Propagations*, Vol. 57, No. 11, 3672–3676, Nov. 2009.
4. Bayderkhani, R. and H. R. Hassani, "Wideband and low sidelobe linear series fed Yagi-like antenna array," *Progress In Electromagnetics Research B*, Vol. 17, 153–167, 2009.
5. Qu, S. W. and Q. Y. Chen, "Dual-antenna system composed of patch array and planar Yagi antenna for elimination of blindness in cellular mobile communications," *Progress In Electromagnetics Research C*, Vol. 21, 87–97, 2011
6. Lin, S., "Novel printed Yagi-Uda antenna with high-gain and broadband," *Progress In Electromagnetics Research Letters*, Vol. 20, 107–117, 2011.
7. Kan, H. K., R. B. Waterhouse, A. M. Abbosh, and M. E. Bialkowski, "Simple broadband planar CPW-fed quasi-Yagi antenna," *IEEE Antennas Wireless and Propagation Letters*, Vol. 6, 18–20, 2007.
8. Ta, S. X., B. Kim, H. Choo, and I. Park, "Slot-line-fed quasi-Yagi antenna," *International Symposium on Antennas, Propagation, and EM Theory*, 307–310, Guangzhou, China, 2010.
9. Woo, D. S., Y. G. Kim, K. W. Kim, and Y. K. Cho, "Design of quasi-Yagi antennas using an ultra-wideband balun," *Microwave and Optical Technology Letters*, Vol. 50, No. 8, 781–784, Aug. 2008.
10. Ma, T., C. Wang, R. Hua, and J. Tsai, "A modified quasi-Yagi antenna with a new compact microstrip-to-coplanar strip transition using artificial transmission lines," *IEEE Transactions on Antennas and Propagation*, Vol. 57, No. 8, 2469–2474, Aug. 2009.
11. Sor, J., Y. Qian, and T. Itoh, "Coplanar waveguide fed Quasi-Yagi antenna," *Electronics Letters*, Vol. 36, No. 1, 1–2, Jan. 2000.
12. Truong, L. H., Y. H. Baek, M. K. Lee, S. W. Park, S. J. Lee, and J. K. Rhee, "A high-performance 94 GHz planar quasi-Yagi antenna on GaAs substrate," *Microwave and Optical Technology Letters*, Vol. 51, No. 10, 2396–2400, Jul. 2009.
13. Chang, D., C. Chang, and J. Liu, "Modified planar quasi-Yagi antenna for WLAN dual-band operations," *Microwave and Optical*

Technology Letters, Vol. 46, No. 8, 443–446, Sep. 2005.

14. Eldek, A. A., "Design of double dipole antenna with enhanced usable bandwidth for wideband phased array applications," *Progress In Electromagnetics Research*, Vol. 59, 1–15, 2006.
15. Steyn, J. M., J. W. Odendaal, and J. Joubert, "Double dipoles antenna for dual-band wireless local area networks applications," *Microwave and Optical Technology Letters*, Vol. 51, No. 9, 2034–784, Sep. 2008.
16. Xin, Q., F. S. Zhang, B. H. Sun, Y. L. Zou, and Q. Z. Liu, "Dual-band Yagi-Uda antenna for wireless communications," *Progress In Electromagnetics Research Letters*, Vol. 16, 119–129, 2010.
17. Wu, S. C. Kang, K. Chen, and J. Tarng, "A multiband quasi-Yagi type antenna," *IEEE Transactions on Antennas and Propagation*, Vol. 58, No. 2, 593–596, Feb. 2010.
18. Eldek, A. A., A. Z. Elsherbeni, and C. E. Smith, "Wide-band modified printed bow-tie antenna with single and dual polarization for C- and X-band applications," *IEEE Transactions on Antennas and Propagation*, Vol. 53, No. 9, 3067–3072, Sep. 2005.
19. Chen, K., X. Chen, and K. Huang, "A novel microstrip dipole antenna with wideband and end-fire properties," *Journal of Electromagnetic Waves and Applications*, Vol. 21, No. 12, 1679–1688, 2007.
20. Eldek, A. A., "Ultrawideband double rhombus antenna with stable radiation patterns for phased array applications," *IEEE Transactions on Antennas and Propagation*, Vol. 55, No. 1, 84–91, Jan. 2007.
21. Han, K., Y. Park, and I. Park, "Broadband CPS-fed Yagi-Uda antenna," *Electronics Letters*, Vol. 45, No. 24, 1207–1209, Dec. 2009.
22. Alhalabi, R. and G. Rebeiz, "Differentially-fed millimeter-wave Yagi-Uda antennas with folded dipole feed," *IEEE Transactions on Antennas and Propagation*, Vol. 58, No. 3, 966–969, Mar. 2010.
23. Zinieris, M. M., R. Sloan, and L. E. Davis, "A broadband microstrip-line-to-slot-line transition," *Microwave and Optical Technology Letters*, Vol. 18, No. 5, 339–342, Aug. 1998.